Transport of tungsten in the H-mode edge transport barrier of ITER

R. Dux[1], E. Fable[1], A. Kukushkin[2], A. Loarte[2], and ASDEX Upgrade team

[1]*Max-Planck-Institut für Plasmaphysik, EURATOM Association, Garching, Germany*

[2]*ITER Organization, Route de Vinon sur Verdon, 13115 Saint Paul Lez Durance, France*

Even though the erosion rates of tungsten (W) are much lower than for the light elements, the risk of high central power losses by radiation is still inherent in the use of W as a divertor material in ITER. The penetration of W into the central plasma depends on many mechanisms: prompt redeposition, transport of W ions parallel to the magnetic field out of the divertor volume, and radial transport across the separatrix and further into the core of the plasma. An important element is the transport in the edge transport barrier (ETB) of H-mode plasmas.

Direct measurements of the impurity transport coefficients in this region were performed in ASDEX Upgrade by analysing the density profile evolution of helium, carbon, neon and argon measured with charge exchange recombination spectroscopy [1]. It was found that between ELMs, all impurities are subject to an inward pinch leading to steep impurity density gradients which are flattened during ELMs. The evaluated impurity transport coefficients between ELMs were in accordance with neoclassical theory and caused an increase in the peaking with increasing impurity charge. Therefore, it can be assumed that W transport in the ETB will be appropriately described by neoclassical theory. In this paper, the neoclassical transport of W is studied for a large range of pedestal profiles of electron density and temperature at various values for plasma current and toroidal field. This is a more methodical approach complementing a previous study for one specific background profile [2].

w_T [cm]	T_{ped} [keV]	T_{sep} [keV]	T_{axis} [keV]	w_n [cm]	n_{ped} [10^{19}m^{-3}]	n_{sep} [n_{ped}]
3,**6**,9	3,**4.5**,6	0.3	22	3,**6**,9	6.5,**8**,9.5	≈0.2-0.8

Table 1: *Parameter ranges for a DT-plasma at I_p=15 MA and B_T=5.3 T.*

Parametric Scan of Pedestal Parameters

The parametrisation of the electron density $n_e(x)$ in the edge pedestal region uses the pedestal density n_{ped}, the separatrix density n_{sep} and the characteristic density pedestal width w_n via:

$$n_e(x) = \frac{n_{ped}+n_{sep}}{2} + \frac{n_{ped}-n_{sep}}{2}\ \frac{\tanh(2x/w_n-1)}{\tanh(1)} \tag{1}$$

Here, the co-ordinate x is the distance to the separatrix as measured at the low-field side on a horizontal chord through the magnetic axis. For the temperature $T(x)$, the parametrisation is identical for $x < w_T$. Just one temperature T=T_e=T_i is used. For the neoclassical transport, only T_i is of importance, while T_e enters indirectly via the charge distribution of tungsten. The mean temperature in ITER is close to T_i at the plasma edge because of the large ratio of the expected energy confinement time to the typical timescale for equipartition. Since T_i is usually above T_e close to the separatrix, a T_{sep} of roughly $1.5\times T_{e,sep}$ was used. $T(x)$ continues as a linearly increasing function further inward.

$$T_{>w_T}(x) = T_{ped} + (T_{axis}-T_{ped})\ \frac{x-w_T}{a-w_T} \quad \text{for } w_T \ll x \tag{2}$$

Here, T_{axis} is the temperature on axis, which is at a distance a to the separatrix. In order to avoid a discontinuity of the temperature gradient at $x = w_T$, we used a smooth transition of the two temperature functions within $w_T/5$ around x=w_T using:

$$T(x) = (1-f(x))T_{<w_T}(x) + f(x)T_{>w_T}(x) \quad \text{with} \quad f(x) = \frac{1+\tanh[10(x/w_T-1)]}{2} \tag{3}$$

For each combination of the toroidal field B_T and plasma current I_p, three values of the pedestal width and height for the density and temperature were studied, so that that 81 combinations of pedestal characteristics were considered per (B_T, I_p). The values considered for a DT-plasma with I_p=15 MA and B_T=5.3 T are shown in Tab.1. For each parameter combination, the neoclassical transport parameters were calculated for ten values of n_{sep}. This procedure was repeated for 5.3 T and 7.5, 10 and 12.5 MA and again for 7.5 MA at half field of 2.65 T representing plasmas with lower heating power in the non-nuclear phase. Here, the values for n_{ped}, T_{ped} and T_{axis} were scaled linearly with I_p and for the separatrix temperature, the scaling was.

$$T_{sep}(I_p,B_T) = T_{sep}(15MA,5.3\mathrm{T})\left(\frac{B_T}{5.3\mathrm{T}}\right)^{4/7}\left(\frac{15\mathrm{MA}}{I_p}\right)^{2/7}\left(\frac{5+10(I_p/15\mathrm{MA})^3}{15}\right)^{2/7} \quad (4)$$

The main ion species is a 50/50 mix of D and T. The calculations were performed with the NEOART code and include impurity-impurity collisions. The necessary flux surface averages of the magnetic field and the trapped particle fraction were calculated from equilibria of ITER plasmas as provided by g-eqdisk files. The chosen impurity composition included He(2%), Be(2%), Ar(0.1%) and W(5×10^{-6}) with radially constant concentration profiles. The charge distribution is approximated by the corona distribution leading to a $Z_{eff}\approx$1.6. Fig.1 shows the pedestal profiles of temperature, density and resulting transport coefficients of tungsten for a 15MA/5.3T case (black line) and a 7.5MA/5.3T case (red dashed lines). The profiles shown in Fig.1 are for the central values of the parameter space, i.e. the bold values in Tab.1 and the appropriately scaled values for the 7.5MA case. For n_{sep}, the values are 3.1×10^{19} m^{-3} and 2.1×10^{19} m^{-3} respectively. The collisionality of W is in the Pfirsch-Schlüter (PS) regime as indicated in the upper right box, where $\nu^*\varepsilon^{3/2}$ is far above the PS-limit of 1. Thus, the collisional transport of W is dominated by the classical and Pfirsch-Schlüter contribution, while the banana-plateau transport is small. The diffusion coefficient rises with collisionality and is on average 1.7 and 4.2×10^{-2} m^{2}s^{-1} for the two cases. The drift velocity v is outward (positive) at the edge, inward around x=5 cm and again outward further in as can be seen from the plot of v/D in the lower middle box. In temporal equilibrium, v/D equals the normalised density gradient of tungsten and the integral of v/D across the radial range of the ETB delivers the ratio of the tungsten densities at the edges of the radial interval

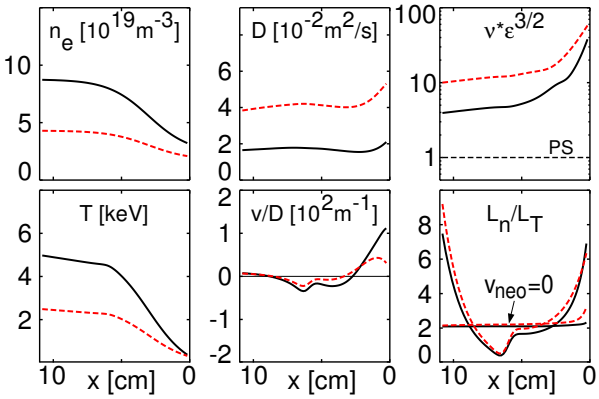

Fig.1: *Pedestal profiles and collisional transport coefficients of W for 15 MA (black) and 7.5 MA (red dashed) at 5.3 T. Density and temperature parameters are as given by the bold values in Tab.1*

$$f_W = \frac{n_W(r_{top})}{n_W(r_{edge})} = \exp\left[\int_{r_{edge}}^{r_{top}} \frac{v\,dr}{D}\right] \quad (5)$$

For the v/D profiles of Fig.1, we obtain f_W=0.32 at 15 MA and 0.38 at 7.5 MA. The drift velocity of tungsten contains the sum of inward pinch contributions proportional to the normalised density gradients of main ions and light impurities and outward contribution proportional to the normalised ion temperature gradient. All normalised ion density gradients are approximately equal to the normalised electron density gradient due to the choice of a constant impurity concentration and due to the mild influence of the argon charge state distribution on the quasi-

neutrality condition which determines the density of the main ions. When using f_{ne} and f_T for the ratios of electron density and ion temperature respectively, we can approximately write for the local value of v/D and the tungsten density ratio which results after integration.

$$\frac{v(r)}{D(r)} \approx \frac{Z_W}{\langle Z_i \rangle}\left(\frac{1}{n_e}\frac{dn_e}{dr} - H\frac{1}{T}\frac{dT}{dr}\right) \qquad \ln(f_W) \approx \frac{\langle Z_W \rangle}{\langle Z_i \rangle}\left(\ln(f_{ne}) - H_{eff}\ln(f_T)\right) \tag{6}$$

The lower right box of Fig.1 shows the ratio of normalised temperature and electron density gradient L_n/L_T for both cases and the critical ratios $1/H$ at which the neoclassical drift velocity of tungsten is zero. The critical ratio is slightly above 2. For regions, where stronger temperature gradients lead to ratios above the critical value, the drift is outward and vice versa. For very high collisionalities, the temperature screening of the PS-contribution is reduced. An indication of this is seen at the edge for the 7.5 MA case, where the critical value for zero drift velocity rises to about 3 due to a reduction of H in eq.(6). When increasing the separatrix density compared to the values of Fig.1, the normalised density gradient decreases and the drift direction will be predominantly outward in the ETB region. Here, a slight decrease of f_{ne} causes a strong decrease of f_W due to the high charge Z_W of tungsten. The scaling exponent is given by $\langle Z_W \rangle / \langle Z_i \rangle$ a properly weighted mean of the tungsten charge in the ETB divided by a weighted mean of the charge of light impurities and main ions. For the above cases, Z_W increases from 19(18) at the edge to 51(42) at the inner boundary and changes of f_{ne} are amplified by an exponent of 14.6(12.0) leading to enormously hollow or peaked equilibrium W profiles in the ETB. This equilibrium peaking of W is just an extrapolation from the neoclassical transport for the given impurity profiles and various non-linear effects would have to be considered using a radial transport calculation for impurities and energy to make a more precise evaluation of its magnitude for ITER.

Scaling of the pedestal parameters leading to flat W-profiles

For each parameter set, the separatrix density was varied in fine steps and the according tungsten density ratio f_W was evaluated using eq.(5) for the interval x=[0.2,9.9] cm. The inner boundary of the calculations was chosen to be large enough to include the total density rise for the case with a large pedestal width of 9 cm. From this variation, the n_{sep} value leading to a flat W-profile (f_W=1) was determined. The second eq.(6) yields, that f_W equals unity when the term in the bracket is zero, i.e. $H_{eff} = \ln(f_{ne})/\ln(f_T)$. Thus, H_{eff} was calculated for all parameter sets from the corresponding electron density and temperature ratios. H_{eff} varies between 0.33 and 0.6. A H_{eff} function, which yields a good fit to the data set, has only a linear dependence on the collisionality of W at the plasma edge plus a correction term that depends on the ratio of density to temperature pedestal width.

$$\begin{aligned} H_{eff} &= H_{av} + \Delta H_{\nu^*} + \Delta H_s \ , \ H_{av} = 0.41 \ , \ \Delta H_{\nu^*} = -4.07\times10^{-2}\left(\frac{B_T n_{sep}}{3.726 \times I_p T_{sep}} - 1\right) \\ \Delta H_s &= \frac{H_s^+ - H_s^-}{2}x_s + \frac{H_s^+ + H_s^-}{2}x_s^2 \quad x_s = \frac{\ln(w_n/w_T)}{\ln(3)} \\ H_s^+ &= -5.89\times10^{-2} \quad H_s^- = 4.92\times10^{-1}(ln(f_T)-1) - 9.51\times10^{-2} ln(f_T)^2 \end{aligned} \tag{7}$$

The ΔH_{ν^*}-term was introduced due to the reduced temperature screening at high collisionalities which only appears at the plasma edge (see Fig.1). However, it causes only a small change between -0.03 at low to 0.03 at high ν^*. Here, $B_T n_{sep}/(I_p T_{sep})$ was used as a proxy for the ν^* variation that only depends on profile parameters (Z_W^2 increases about linearly with T such that the usual $1/T^2$-scaling is replaced by $1/T$). The units in eq.(7) are $[I_p]$=MA, $[B_T]$=T, $[n_{sep}]$=10^{19}m^{-3} and $[T_{sep}]$=keV. The shape correction ΔH_s is zero for w_n=w_T, it reduces to H_s^+=-0.06 at w_n=3w_T and increases for lower density widths up to H_s^-=0.06-0.14 for w_n=$w_T/3$.

H_s^- is lowest for low values of f_T. ΔH_s is caused by the increase of Z_W with temperature. For w_n<w_T, the inward pinch term in eq.(6) appears at a radius where Z_W is still relatively low and thus has a lower weight in the integral of eq.(5) than the outward directed T_i-gradient term which enters with higher values of Z_W in the integral. The relative deviation of the fitted f_{ne} from the data is between -5.3% and 4.7% and the absolute value of this deviation is on average 1.6%. When only using H_{av}, the deviations are up to 38%. Finally, the fit function can be used to calculate $n_{sep}(f_W{=}1)$ for any parameter set. To this end, f_T is computed via eq.(2) and eq.(3) from the temperature parameters and then the corresponding H_{eff}, which is first evaluated without the ΔH_{v^*}-correction, delivers f_{ne} and via eq.(1) a starting value for n_{sep}. In the next iterations, the ΔH_{v^*}-correction is included taking n_{sep} from the previous iteration, which quickly converges to the final value for $n_{sep}(f_W{=}1)$. Fig.2 shows colour maps of these separatrix densities for 15MA/5.3T and for 7.5MA/2.65T as a function of T_{ped} and n_{ped} for all settings of the width-parameters w_n and w_T. In the colour scales, the black lines with uncertainty interval indicate the minimum values for n_{sep} (3-4$\times10^{-19}$m^{-3} for 15MA/5.3T and 1.5-2$\times10^{-19}$m^{-3} for 7.5MA/2.65T) which have to be achieved to control the power exhaust in ITER [3, 4]. The prevailing part of the scanned parameter space requires lower n_{sep} values to get into the regime of outward drift dominated W-transport as can be seen from the areas below the black lines in the individual colour maps. Only for a wide density and narrow temperature pedestal profile, about half of the parameter combinations lead to a situation with a dominant neoclassical inward pinch.

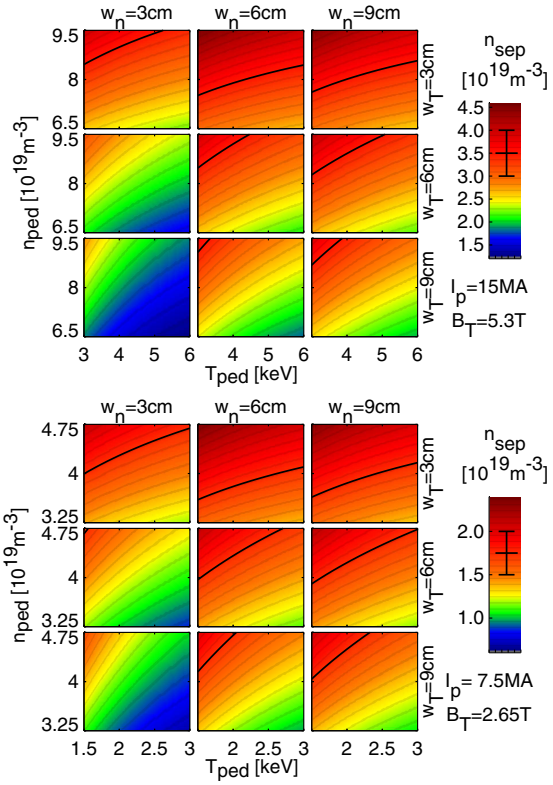

Fig.2: *Separatrix densities leading to equal tungsten densities at the edge and the pedestal top. For higher n_{sep} values, neoclassical transport provokes hollow W-profiles and vice versa. The black lines give an estimate of the minimum n_{sep} values being required to control the power exhaust (uncertainty interval is shown in the colour scale). Thus, all parameter combinations leading to a colour below this minimum value have an outward drift dominated W-transport in the ETB and vice versa.*

Independent of whether the W profiles in the ETB would be hollow or peaked in equilibrium, the timescale for the evolution towards equilibrium is long due to the small neoclassical transport coefficients (see Fig.1). Therefore, an ELM frequency above 10 Hz would be sufficient to flatten the expected hollow W profiles. Such controlled ELM frequencies should be easily achieved with the ITER schemes for ELM control. To verify this, radial transport calculations were done and will be soon reported elsewhere.

Disclaimer: The views and opinions expressed herein do not necessarily reflect those of the ITER Organization

References

[1] T. Pütterich et al, J. Nuc. Mat. **415** (2011) 334.
[2] R. Dux et al, Nucl. Fus. **51** (2011) 053002.
[3] A. Kukushkin et al, 23rd IAEA-Fusion Energy Conf. IAEA-CN-180, (2010) ITR/P1-33.
[4] A. Kukushkin et al, 24th IAEA-Fusion Energy Conf. IAEA-CN-197, (2012) ITR/P1-27.